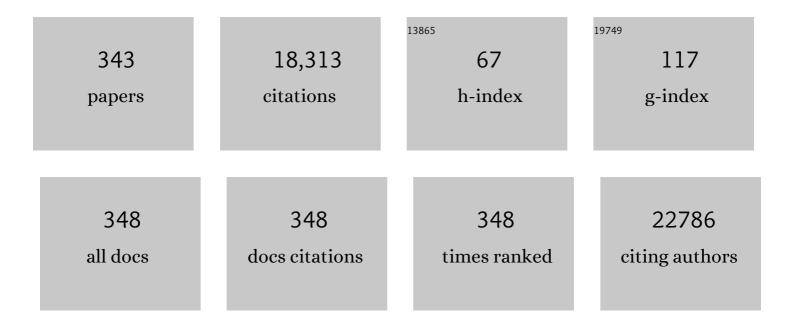
## Jamie H Warner

List of Publications by Year in descending order

Source: https://exaly.com/author-pdf/3003794/publications.pdf

Version: 2024-02-01



IAMIE H WADNED

#	Article	IF	CITATIONS
1	Atomically sharp jagged edges of chemical vapor deposition-grown WS2 for electrocatalysis. Materials Today Nano, 2022, 18, 100183.	4.6	5
2	Wafer-Scalable Single-Layer Amorphous Molybdenum Trioxide. ACS Nano, 2022, 16, 3756-3767.	14.6	16
3	Elucidating the Formation and Structural Evolution of Platinum Single-Site Catalysts for the Hydrogen Evolution Reaction. ACS Catalysis, 2022, 12, 3173-3180.	11.2	18
4	Ultrathin Lateral 2D Photodetectors Using Transition-Metal Dichalcogenides PtSe <sub>2</sub> –WS <sub>2</sub> –PtSe <sub>2</sub> by Direct Laser Patterning. ACS Applied Electronic Materials, 2022, 4, 1029-1038.	4.3	4
5	Mapping 1D Confined Electromagnetic Edge States in 2D Monolayer Semiconducting MoS <sub>2</sub> Using 4D-STEM. ACS Nano, 2022, 16, 6657-6665.	14.6	9
6	Atomic-Level Dynamics of Point Vacancies and the Induced Stretched Defects in 2D Monolayer PtSe <sub>2</sub> . Nano Letters, 2022, 22, 3289-3297.	9.1	9
7	Atomic-Scale Insights into the Lateral and Vertical Epitaxial Growth in Two-Dimensional Pd <sub>2</sub> Se <sub>3</sub> –MoS <sub>2</sub> Heterostructures. ACS Nano, 2022, 16, 10260-10272.	14.6	3
8	Recent Progress in Using Graphene as an Ultrathin Transparent Support for Transmission Electron Microscopy. Small Structures, 2021, 2, 2000049.	12.0	19
9	High-performance magnesium metal batteries <i>via</i> switching the passivation film into a solid electrolyte interphase. Energy and Environmental Science, 2021, 14, 4391-4399.	30.8	49
10	A System-Agnostic, Adaptable and Extensible Animal Support Cradle System for Cardio-Respiratory-Synchronised, and Other, Multi-Modal Imaging of Small Animals. Tomography, 2021, 7, 39-54.	1.8	1
11	Unraveling the Intricacies of Residual Lithium in High-Ni Cathodes for Lithium-Ion Batteries. ACS Energy Letters, 2021, 6, 941-948.	17.4	86
12	Nanoscale Bilayer Mechanical Lithography Using Water as Developer. Nano Letters, 2021, 21, 3827-3834.	9.1	2
13	Atomically Precise Control of Carbon Insertion into hBN Monolayer Point Vacancies using a Focused Electron Beam Guide. Small, 2021, 17, e2100693.	10.0	13
14	Intrinsic Li Distribution in Layered Transition-Metal Oxides Using Low-Dose Scanning Transmission Electron Microscopy and Spectroscopy. Chemistry of Materials, 2021, 33, 4638-4650.	6.7	7
15	Wet-CO <sub>2</sub> Pretreatment Process for Reducing Residual Lithium in High-Nickel Layered Oxides for Lithium-Ion Batteries. ACS Applied Materials & Interfaces, 2021, 13, 27096-27105.	8.0	23
16	Inâ€Depth Analysis of the Degradation Mechanisms of Highâ€Nickel, Low/Noâ€Cobalt Layered Oxide Cathodes for Lithiumâ€Ion Batteries. Advanced Energy Materials, 2021, 11, 2100858.	19.5	79
17	Atomic Study on Defects in 2D PtSe2 Monolayers Using Electron Microscopy. Microscopy and Microanalysis, 2021, 27, 644-645.	0.4	0
18	Large-Scale Uniform-Patterned Arrays of Ultrathin All-2D Vertical Stacked Photodetector Devices. ACS Applied Materials & Interfaces, 2021, 13, 34696-34704.	8.0	2

#	Article	IF	CITATIONS
19	Rational Design of Coating Ions via Advantageous Surface Reconstruction in Highâ€Nickel Layered Oxide Cathodes for Lithiumâ€Ion Batteries. Advanced Energy Materials, 2021, 11, 2101112.	19.5	58
20	Atomic Structure of Dislocations and Grain Boundaries in Two-Dimensional PtSe <sub>2</sub> . ACS Nano, 2021, 15, 16748-16759.	14.6	12
21	Thick BaTiO <sub>3</sub> Epitaxial Films Integrated on Si by RF Sputtering for Electro-Optic Modulators in Si Photonics. ACS Applied Materials & Interfaces, 2021, 13, 51230-51244.	8.0	20
22	Atomistic Mechanics of Torn Back Folded Edges of Triangular Voids in Monolayer WS <sub>2</sub> . Small, 2021, 17, e2104238.	10.0	3
23	GaS:WS <sub>2</sub> Heterojunctions for Ultrathin Two-Dimensional Photodetectors with Large Linear Dynamic Range across Broad Wavelengths. ACS Nano, 2021, 15, 19570-19580.	14.6	20
24	Controlling Defects in Continuous 2D GaS Films for Highâ€Performance Wavelengthâ€Tunable UVâ€Discriminating Photodetectors. Advanced Materials, 2020, 32, e1906958.	21.0	53
25	Direct Imaging of Individual Molecular Binding to Clean Nanopore Edges in 2D Monolayer MoS <sub>2</sub> . ACS Nano, 2020, 14, 153-165.	14.6	19
26	Controlling Photoluminescence Enhancement and Energy Transfer in WS <sub>2</sub> :hBN:WS <sub>2</sub> Vertical Stacks by Precise Interlayer Distances. Small, 2020, 16, e1905985.	10.0	26
27	Atomic structure of defects in transitional metal dichalcogenides using transmission electron microscopy. , 2020, , 167-197.		3
28	Selfâ€Assembly of Bowlic Supramolecules on Graphene Imaged at the Individual Molecular Level using Heavy Atom Tagging. Small, 2020, 16, e2002860.	10.0	8
29	Single-Step Chemical Vapor Deposition Growth of Platinum Nanocrystal: Monolayer MoS <sub>2</sub> Dendrite Hybrid Materials for Efficient Electrocatalysis. Chemistry of Materials, 2020, 32, 8243-8256.	6.7	23
30	Electromagnetically Transparent Graphene Respiratory Sensors for Multimodal Small Animal Imaging. Advanced Healthcare Materials, 2020, 9, 2001222.	7.6	4
31	A Metal-Free Oxygenated Covalent Triazine 2-D Photocatalyst Works Effectively from the Ultraviolet to Near-Infrared Spectrum for Water Oxidation Apart from Water Reduction. ACS Applied Energy Materials, 2020, 3, 8960-8968.	5.1	7
32	Phase Variations and Layer Epitaxy of 2D PdSe <sub>2</sub> Grown on 2D Monolayers by Direct Selenization of Molecular Pd Precursors. ACS Nano, 2020, 14, 11677-11690.	14.6	10
33	Microscopic Mechanism of Van der Waals Heteroepitaxy in the Formation of MoS2/hBN Vertical Heterostructures. ACS Omega, 2020, 5, 31692-31699.	3.5	5
34	In-Situ Atomic Level Studies of Unusual Phase Transformations in Metal-chalcogenide 2D Crystals. Microscopy and Microanalysis, 2020, 26, 1084-1085.	0.4	0
35	Atomic Structure and Dynamics of Defects and Grain Boundaries in 2D Pd2Se3 Monolayers. Microscopy and Microanalysis, 2020, 26, 1636-1640.	0.4	0
36	Operational Limits and Failure Mechanisms in All-2D van der Waals Vertical Heterostructure Devices with Long-Lived Persistent Electroluminescence. ACS Nano, 2020, 14, 15533-15543.	14.6	7

#	Article	IF	CITATIONS
37	Transparent ultrathin all-two-dimensional lateral Gr:WS2:Gr photodetector arrays on flexible substrates and their strain induced failure mechanisms. Materials Today Advances, 2020, 6, 100067.	5.2	7
38	Synthesis and Applications of Wide Bandgap 2D Layered Semiconductors Reaching the Green and Blue Wavelengths. ACS Applied Electronic Materials, 2020, 2, 1777-1814.	4.3	50
39	2D layered noble metal dichalcogenides (Pt, Pd, Se, S) for electronics and energy applications. Materials Today Advances, 2020, 7, 100076.	5.2	55
40	Direct observation and catalytic role of mediator atom in 2D materials. Science Advances, 2020, 6, eaba4942.	10.3	7
41	In situ atomic level studies of thermally controlled interlayer stacking shifts in 2D transition metal dichalcogenide bilayers. Journal of Materials Research, 2020, 35, 1407-1416.	2.6	0
42	Precursor Design for High Density Single Pt Atom Sites on MoS <sub>2</sub> : Enhanced Stability at Elevated Temperatures and Reduced 3D Clustering. Chemistry of Materials, 2020, 32, 2541-2551.	6.7	8
43	Photoresponse-Bias Modulation of a High-Performance MoS <sub>2</sub> Photodetector with a Unique Vertically Stacked 2H-MoS <sub>2</sub> /1T@2H-MoS <sub>2</sub> Structure. ACS Applied Materials & Interfaces, 2020, 12, 33325-33335.	8.0	76
44	Atomic structure and defect dynamics of monolayer lead iodide nanodisks with epitaxial alignment on graphene. Nature Communications, 2020, 11, 823.	12.8	31
45	Spatially Bandgap-Graded MoS2(1â^'x)Se2x Homojunctions for Self-Powered Visible–Near-Infrared Phototransistors. Nano-Micro Letters, 2020, 12, 26.	27.0	22
46	Simultaneous Identification of Low and High Atomic Number Atoms in Monolayer 2D Materials Using 4D Scanning Transmission Electron Microscopy. Nano Letters, 2019, 19, 6482-6491.	9.1	36
47	Morphology Control of Two-Dimensional Tin Disulfide on Transition Metal Dichalcogenides Using Chemical Vapor Deposition for Nanoelectronic Applications. ACS Applied Nano Materials, 2019, 2, 4222-4231.	5.0	21
48	Postgrowth Substitutional Tin Doping of 2D WS <sub>2</sub> Crystals Using Chemical Vapor Deposition. ACS Applied Materials & Interfaces, 2019, 11, 24279-24288.	8.0	24
49	Striated 2D Lattice with Subâ€nm 1D Etch Channels by Controlled Thermally Induced Phase Transformations of PdSe <sub>2</sub> . Advanced Materials, 2019, 31, e1904251.	21.0	31
50	Contiguous and Atomically Thin Pt Film with Supraâ€Bulk Behavior Through Grapheneâ€Imposed Epitaxy. Advanced Functional Materials, 2019, 29, 1902274.	14.9	22
51	Photocurrent Direction Control and Increased Photovoltaic Effects in All-2D Ultrathin Vertical Heterostructures Using Asymmetric h-BN Tunneling Barriers. ACS Applied Materials & Interfaces, 2019, 11, 40274-40282.	8.0	10
52	Atomically Sharp Dual Grain Boundaries in 2D WS <sub>2</sub> Bilayers. Small, 2019, 15, e1902590.	10.0	13
53	Strong Opto-Structural Coupling in Low Dimensional GeSe <sub>3</sub> Films. Nano Letters, 2019, 19, 7377-7384.	9.1	11
54	Atomic Structure and Dynamics of Epitaxial Platinum Bilayers on Graphene. ACS Nano, 2019, 13, 12162-12170.	14.6	15

4

#	Article	IF	CITATIONS
55	Broadband transparent optical phase change materials for high-performance nonvolatile photonics. Nature Communications, 2019, 10, 4279.	12.8	349
56	Waterproof molecular monolayers stabilize 2D materials. Proceedings of the National Academy of Sciences of the United States of America, 2019, 116, 20844-20849.	7.1	32
57	In situ high temperature atomic level dynamics of large inversion domain formations in monolayer MoS2. Nanoscale, 2019, 11, 1901-1913.	5.6	19
58	Atomic Scale Imaging of Reversible Ring Cyclization in Graphene Nanoconstrictions. ACS Nano, 2019, 13, 2379-2388.	14.6	3
59	High Photoresponsivity in Ultrathin 2D Lateral Graphene:WS <sub>2</sub> :Graphene Photodetectors Using Direct CVD Growth. ACS Applied Materials & Interfaces, 2019, 11, 6421-6430.	8.0	78
60	Thermal Degradation of Monolayer MoS2 on SrTiO3 Supports. Journal of Physical Chemistry C, 2019, 123, 3876-3885.	3.1	17
61	Metal Atom Markers for Imaging Epitaxial Molecular Self-Assembly on Graphene by Scanning Transmission Electron Microscopy. ACS Nano, 2019, 13, 7252-7260.	14.6	13
62	Atomic Structure and Dynamics of Defects and Grain Boundaries in 2D Pd <sub>2</sub> Se <sub>3</sub> Monolayers. ACS Nano, 2019, 13, 8256-8264.	14.6	38
63	Atomic structural catalogue of defects and vertical stacking in 2H/3R mixed polytype multilayer WS <sub>2</sub> pyramids. Nanoscale, 2019, 11, 10859-10871.	5.6	3
64	Increasing the electrochemical activity of basal plane sites in porous 3D edge rich MoS2 thin films for the hydrogen evolution reaction. Materials Today Energy, 2019, 13, 134-144.	4.7	31
65	Anisotropic Fracture Dynamics Due to Local Lattice Distortions. ACS Nano, 2019, 13, 5693-5702.	14.6	19
66	High-Performance WS <sub>2</sub> Monolayer Light-Emitting Tunneling Devices Using 2D Materials Grown by Chemical Vapor Deposition. ACS Nano, 2019, 13, 4530-4537.	14.6	56
67	Grain Boundaries as Electrical Conduction Channels in Polycrystalline Monolayer WS <sub>2</sub> . ACS Applied Materials & Interfaces, 2019, 11, 10189-10197.	8.0	17
68	Atomic electrostatic maps of 1D channels in 2D semiconductors using 4D scanning transmission electron microscopy. Nature Communications, 2019, 10, 1127.	12.8	62
69	Atomic Resolution Defocused Electron Ptychography at Low Dose with a Fast, Direct Electron Detector. Scientific Reports, 2019, 9, 3919.	3.3	44
70	MoS <sub>2</sub> Liquid Cell Electron Microscopy Through Clean and Fast Polymer-Free MoS <sub>2</sub> Transfer. Nano Letters, 2019, 19, 1788-1795.	9.1	45
71	Biomass-Derived Nickel Phosphide Nanoparticles as a Robust Catalyst for Hydrogen Production by Catalytic Decomposition of C <sub>2</sub> H <sub>2</sub> or Dry Reforming of CH <sub>4</sub> . ACS Applied Energy Materials, 2019, 2, 8649-8658.	5.1	11
72	In-Situ Atomic-Scale Dynamics of Thermally Driven Phase Transition of 2D Few-Layered 1T PtSe <sub>2</sub> into Ultrathin 2D Nonlayered PtSe Crystals. Chemistry of Materials, 2019, 31, 9895-9903.	6.7	25

#	Article	IF	CITATIONS
73	Ultrathin All-2D Lateral Graphene/GaS/Graphene UV Photodetectors by Direct CVD Growth. ACS Applied Materials & Interfaces, 2019, 11, 48172-48178.	8.0	30
74	Direct Laser Patterning and Phase Transformation of 2D PdSe2 Films for On-Demand Device Fabrication. ACS Nano, 2019, 13, 14162-14171.	14.6	44
75	Spatially Controlled Fabrication and Mechanisms of Atomically Thin Nanowell Patterns in Bilayer WS <sub>2</sub> Using <i>in Situ</i> High Temperature Electron Microscopy. ACS Nano, 2019, 13, 14486-14499.	14.6	14
76	Self-Limiting Growth of High-Quality 2D Monolayer MoS <sub>2</sub> by Direct Sulfurization Using Precursor-Soluble Substrates for Advanced Field-Effect Transistors and Photodetectors. ACS Applied Nano Materials, 2019, 2, 369-378.	5.0	27
77	Symmetry-Controlled Reversible Photovoltaic Current Flow in Ultrathin All 2D Vertically Stacked Graphene/MoS <sub>2</sub> /WS <sub>2</sub> /Graphene Devices. ACS Applied Materials & Interfaces, 2019, 11, 2234-2242.	8.0	32
78	Synthesis of Surface Grown Pt Nanoparticles on Edge-Enriched MoS <sub>2</sub> Porous Thin Films for Enhancing Electrochemical Performance. Chemistry of Materials, 2019, 31, 387-397.	6.7	40
79	Electrocatalytic Volleyball: Rapid Nanoconfined Nicotinamide Cycling for Organic Synthesis in Electrode Pores. Angewandte Chemie, 2019, 131, 5002-5006.	2.0	5
80	Electrocatalytic Volleyball: Rapid Nanoconfined Nicotinamide Cycling for Organic Synthesis in Electrode Pores. Angewandte Chemie - International Edition, 2019, 58, 4948-4952.	13.8	60
81	Addressing the isomer cataloguing problem for nanopores in two-dimensional materials. Nature Materials, 2019, 18, 129-135.	27.5	57
82	Direct Imaging of Photoswitching Molecular Conformations Using Individual Metal Atom Markers. ACS Nano, 2019, 13, 87-96.	14.6	22
83	Revealing Strain-Induced Effects in Ultrathin Heterostructures at the Nanoscale. Nano Letters, 2018, 18, 2467-2474.	9.1	22
84	Utilizing Interlayer Excitons in Bilayer WS <sub>2</sub> for Increased Photovoltaic Response in Ultrathin Graphene Vertical Cross-Bar Photodetecting Tunneling Transistors. ACS Nano, 2018, 12, 4669-4677.	14.6	37
85	Epitaxial and atomically thin graphene–metal hybrid catalyst films: the dual role of graphene as the support and the chemically-transparent protective cap. Energy and Environmental Science, 2018, 11, 1610-1616.	30.8	34
86	High-Performance All 2D-Layered Tin Disulfide: Graphene Photodetecting Transistors with Thickness-Controlled Interface Dynamics. ACS Applied Materials & Interfaces, 2018, 10, 13002-13010.	8.0	32
87	Determining the Optimized Interlayer Separation Distance in Vertical Stacked 2D WS <sub>2</sub> :hBN:MoS <sub>2</sub> Heterostructures for Exciton Energy Transfer. Small, 2018, 14, e1703727.	10.0	54
88	Hydrogen-Assisted Growth of Large-Area Continuous Films of MoS <sub>2</sub> on Monolayer Graphene. ACS Applied Materials & Interfaces, 2018, 10, 7304-7314.	8.0	47
89	Atomic Resolution Imaging of Nanoscale Chemical Expansion in Pr <sub><i>x</i></sub> Ce <sub>1–<i>x</i></sub> O <sub>2â^î^</sub> during <i>In Situ</i> Heating. ACS Nano, 2018, 12, 1359-1372.	14.6	8
90	Large Dendritic Monolayer MoS <sub>2</sub> Grown by Atmospheric Pressure Chemical Vapor Deposition for Electrocatalysis. ACS Applied Materials & Interfaces, 2018, 10, 4630-4639.	8.0	88

#	Article	IF	CITATIONS
91	Interlocking Friction Governs the Mechanical Fracture of Bilayer MoS <sub>2</sub> . ACS Nano, 2018, 12, 3600-3608.	14.6	40
92	Geometrically Enhanced Thermoelectric Effects in Graphene Nanoconstrictions. Nano Letters, 2018, 18, 7719-7725.	9.1	46
93	Epitaxial Growth of Monolayer MoS <sub>2</sub> on SrTiO <sub>3</sub> Single Crystal Substrates for Applications in Nanoelectronics. ACS Applied Nano Materials, 2018, 1, 6976-6988.	5.0	34
94	2D-Layer-Dependent Behavior in Lateral Au/WS <sub>2</sub> /Graphene Photodiode Devices with Optical Modulation of Schottky Barriers. ACS Applied Nano Materials, 2018, 1, 6874-6881.	5.0	22
95	Nanoporous Graphene: Facile Fabrication of Large-Area Atomically Thin Membranes by Direct Synthesis of Graphene with Nanoscale Porosity (Adv. Mater. 49/2018). Advanced Materials, 2018, 30, 1870376.	21.0	1
96	Facile Fabrication of Largeâ€Area Atomically Thin Membranes by Direct Synthesis of Graphene with Nanoscale Porosity. Advanced Materials, 2018, 30, e1804977.	21.0	56
97	Hollow Electron Ptychographic Diffractive Imaging. Physical Review Letters, 2018, 121, 146101.	7.8	27
98	<i>In Situ</i> Atomic-Level Studies of Gd Atom Release and Migration on Graphene from a Metallofullerene Precursor. ACS Nano, 2018, 12, 10439-10451.	14.6	9
99	Atomic Structure and Dynamics of Self-Limiting Sub-Nanometer Pores in Monolayer WS <sub>2</sub> . ACS Nano, 2018, 12, 11638-11647.	14.6	30
100	Inhomogeneous Strain Release during Bending of WS <sub>2</sub> on Flexible Substrates. ACS Applied Materials & Interfaces, 2018, 10, 39177-39186.	8.0	17
101	High-Performance Two-Dimensional Schottky Diodes Utilizing Chemical Vapour Deposition-Grown Graphene–MoS <sub>2</sub> Heterojunctions. ACS Applied Materials & Interfaces, 2018, 10, 37258-37266.	8.0	30
102	Atomically sharp interlayer stacking shifts at anti-phase grain boundaries in overlapping MoS <sub>2</sub> secondary layers. Nanoscale, 2018, 10, 16692-16702.	5.6	22
103	Preferential Pt Nanocluster Seeding at Grain Boundary Dislocations in Polycrystalline Monolayer MoS <sub>2</sub> . ACS Nano, 2018, 12, 5626-5636.	14.6	27
104	Atomic structure of defects and dopants in 2D layered transition metal dichalcogenides. Chemical Society Reviews, 2018, 47, 6764-6794.	38.1	178
105	Blister-based-laser-induced-forward-transfer: a non-contact, dry laser-based transfer method for nanomaterials. Nanotechnology, 2018, 29, 385301.	2.6	14
106	Chemical Vapor Deposition Growth of Two-Dimensional Monolayer Gallium Sulfide Crystals Using Hydrogen Reduction of Ga <sub>2</sub> S <sub>3</sub> . ACS Omega, 2018, 3, 7897-7903.	3.5	35
107	Ultralong 1D Vacancy Channels for Rapid Atomic Migration during 2D Void Formation in Monolayer MoS <sub>2</sub> . ACS Nano, 2018, 12, 7721-7730.	14.6	54
108	Low-Frequency Noise in Graphene Tunnel Junctions. ACS Nano, 2018, 12, 9451-9460.	14.6	22

#	Article	IF	CITATIONS
109	Nanoporous Silicon-Assisted Patterning of Monolayer MoS <sub>2</sub> with Thermally Controlled Porosity: A Scalable Method for Diverse Applications. ACS Applied Nano Materials, 2018, 1, 3548-3556.	5.0	3
110	Graphene as a flexible template for controlling magnetic interactions between metal atoms. Journal of Physics Condensed Matter, 2017, 29, 085001.	1.8	1
111	Electrically tunable organic–inorganic hybrid polaritons with monolayer WS2. Nature Communications, 2017, 8, 14097.	12.8	53
112	Oligomeric aminoborane precursors for the chemical vapour deposition growth of few-layer hexagonal boron nitride. CrystEngComm, 2017, 19, 285-294.	2.6	41
113	Atomic Structure and Dynamics of Single Platinum Atom Interactions with Monolayer MoS <sub>2</sub> . ACS Nano, 2017, 11, 3392-3403.	14.6	126
114	MoS2 monolayer catalyst doped with isolated Co atoms for the hydrodeoxygenation reaction. Nature Chemistry, 2017, 9, 810-816.	13.6	683
115	Distinguishing Lead and Molecule States in Graphene-Based Single-Electron Transistors. ACS Nano, 2017, 11, 5325-5331.	14.6	48
116	Transfer of photosynthetic NADP <sup>+</sup> /NADPH recycling activity to a porous metal oxide for highly specific, electrochemically-driven organic synthesis. Chemical Science, 2017, 8, 4579-4586.	7.4	74
117	Hydrogen Addition for Centimeter-Sized Monolayer Tungsten Disulfide Continuous Films by Ambient Pressure Chemical Vapor Deposition. Chemistry of Materials, 2017, 29, 4904-4911.	6.7	49
118	Three dimensional hybrid multi-layered graphene–CNT catalyst supports via rapid thermal annealing of nickel acetate. Journal of Materials Chemistry A, 2017, 5, 10457-10469.	10.3	12
119	Scaling Limits of Graphene Nanoelectrodes. Nano Letters, 2017, 17, 3688-3693.	9.1	40
120	Atomic structure and formation mechanism of sub-nanometer pores in 2D monolayer MoS <sub>2</sub> . Nanoscale, 2017, 9, 6417-6426.	5.6	54
121	Photoluminescence Segmentation within Individual Hexagonal Monolayer Tungsten Disulfide Domains Grown by Chemical Vapor Deposition. ACS Applied Materials & Interfaces, 2017, 9, 15005-15014.	8.0	59
122	Fabrication, Pressure Testing, and Nanopore Formation of Single-Layer Graphene Membranes. Journal of Physical Chemistry C, 2017, 121, 14312-14321.	3.1	39
123	Epitaxial Templating of Two-Dimensional Metal Chloride Nanocrystals on Monolayer Molybdenum Disulfide. ACS Nano, 2017, 11, 6404-6415.	14.6	20
124	Edge-Enriched 2D MoS <sub>2</sub> Thin Films Grown by Chemical Vapor Deposition for Enhanced Catalytic Performance. ACS Catalysis, 2017, 7, 877-886.	11.2	123
125	Field-Effect Control of Graphene–Fullerene Thermoelectric Nanodevices. Nano Letters, 2017, 17, 7055-7061.	9.1	61
126	Photoluminescent Arrays of Nanopatterned Monolayer MoS <sub>2</sub> . Advanced Functional Materials, 2017, 27, 1703688.	14.9	35

#	Article	IF	CITATIONS
127	Lateral Grapheneâ€Contacted Vertically Stacked WS <sub>2</sub> /MoS <sub>2</sub> Hybrid Photodetectors with Large Gain. Advanced Materials, 2017, 29, 1702917.	21.0	111
128	Orientation dependent interlayer stacking structure in bilayer MoS <sub>2</sub> domains. Nanoscale, 2017, 9, 13060-13068.	5.6	19
129	Point defects in turbostratic stacked bilayer graphene. Nanoscale, 2017, 9, 13725-13730.	5.6	12
130	Electrical Breakdown of Suspended Mono- and Few-Layer Tungsten Disulfide <i>via</i> Sulfur Depletion Identified by <i>in Situ</i> Atomic Imaging. ACS Nano, 2017, 11, 9435-9444.	14.6	16
131	Snapshot 3D Electron Imaging of Structural Dynamics. Scientific Reports, 2017, 7, 10839.	3.3	10
132	Growth of Large Single-Crystalline Monolayer Hexagonal Boron Nitride by Oxide-Assisted Chemical Vapor Deposition. Chemistry of Materials, 2017, 29, 6252-6260.	6.7	60
133	Atomically Flat Zigzag Edges in Monolayer MoS <sub>2</sub> by Thermal Annealing. Nano Letters, 2017, 17, 5502-5507.	9.1	70
134	<i>In Situ</i> Atomic-Scale Studies of the Formation of Epitaxial Pt Nanocrystals on Monolayer Molybdenum Disulfide. ACS Nano, 2017, 11, 9057-9067.	14.6	27
135	Atomic Structure and Dynamics of Defects in 2D MoS <sub>2</sub> Bilayers. ACS Omega, 2017, 2, 3315-3324.	3.5	32
136	Aberration measurement of the probe-forming system of an electron microscope using two-dimensional materials. Ultramicroscopy, 2017, 182, 195-204.	1.9	5
137	Hyperfine and Spin-Orbit Coupling Effects on Decay of Spin-Valley States in a Carbon Nanotube. Physical Review Letters, 2017, 118, 177701.	7.8	11
138	Chemistry and Structure of Graphene Oxide <i>via</i> Direct Imaging. ACS Nano, 2016, 10, 7515-7522.	14.6	159
139	Lowâ€Temperature Chemical Vapor Deposition Synthesis of Pt–Co Alloyed Nanoparticles with Enhanced Oxygen Reduction Reaction Catalysis. Advanced Materials, 2016, 28, 7115-7122.	21.0	156
140	Negative Electro-conductance in Suspended 2D WS <sub>2</sub> Nanoscale Devices. ACS Applied Materials & Interfaces, 2016, 8, 32963-32970.	8.0	10
141	Electron-Driven Metal Oxide Effusion and Graphene Gasification at Room Temperature. ACS Nano, 2016, 10, 6323-6330.	14.6	15
142	Generalized Mechanistic Model for the Chemical Vapor Deposition of 2D Transition Metal Dichalcogenide Monolayers. ACS Nano, 2016, 10, 4330-4344.	14.6	190
143	Detailed Atomic Reconstruction of Extended Line Defects in Monolayer MoS <sub>2</sub> . ACS Nano, 2016, 10, 5419-5430.	14.6	161
144	Dynamic Behavior of Single Fe Atoms Embedded in Graphene. Journal of Physical Chemistry C, 2016, 120, 21998-22003.	3.1	25

#	Article	IF	CITATIONS
145	Atomically Sharp Crack Tips in Monolayer MoS <sub>2</sub> and Their Enhanced Toughness by Vacancy Defects. ACS Nano, 2016, 10, 9831-9839.	14.6	130
146	<i>In Situ</i> High Temperature Atomic Level Studies of Large Closed Grain Boundary Loops in Graphene. ACS Nano, 2016, 10, 9165-9173.	14.6	23
147	Alloyed Nanoparticles: Low-Temperature Chemical Vapor Deposition Synthesis of Pt-Co Alloyed Nanoparticles with Enhanced Oxygen Reduction Reaction Catalysis (Adv. Mater. 33/2016). Advanced Materials, 2016, 28, 7292-7292.	21.0	1
148	<i>In Situ</i> Atomic Level Dynamics of Heterogeneous Nucleation and Growth of Graphene from Inorganic Nanoparticle Seeds. ACS Nano, 2016, 10, 9397-9410.	14.6	11
149	Ultrathin 2D Photodetectors Utilizing Chemical Vapor Deposition Grown WS <sub>2</sub> With Graphene Electrodes. ACS Nano, 2016, 10, 7866-7873.	14.6	264
150	Photoinduced Schottky Barrier Lowering in 2D Monolayer WS <sub>2</sub> Photodetectors. Advanced Optical Materials, 2016, 4, 1573-1581.	7.3	62
151	Atomic Structure and Spectroscopy of Single Metal (Cr, V) Substitutional Dopants in Monolayer MoS <sub>2</sub> . ACS Nano, 2016, 10, 10227-10236.	14.6	96
152	Atomic Structure and Dynamics of Epitaxial 2D Crystalline Gold on Graphene at Elevated Temperatures. ACS Nano, 2016, 10, 10418-10427.	14.6	29
153	Importance of the structural integrity of a carbon conjugated mediator for photocatalytic hydrogen generation from water over a CdS–carbon nanotube–MoS <sub>2</sub> composite. Chemical Communications, 2016, 52, 13596-13599.	4.1	20
154	Suppressed Hysteretic Field Emission from Polymer Encapsulated Silver Nanowires. IEEE Nanotechnology Magazine, 2016, , 1-1.	2.0	0
155	Porous Graphene Layers on Pt Catalyst for Long-Term Stability of Fuel Cell Electrode. ECS Transactions, 2016, 75, 837-840.	0.5	0
156	Direct manufacturing of ultrathin graphite on three-dimensional nanoscale features. Scientific Reports, 2016, 6, 22700.	3.3	10
157	Quantum Interference in Graphene Nanoconstrictions. Nano Letters, 2016, 16, 4210-4216.	9.1	70
158	Revealing Defect-State Photoluminescence in Monolayer WS <sub>2</sub> by Cryogenic Laser Processing. ACS Nano, 2016, 10, 5847-5855.	14.6	91
159	Substrate control for large area continuous films of monolayer MoS <sub>2</sub> by atmospheric pressure chemical vapor deposition. Nanotechnology, 2016, 27, 085604.	2.6	69
160	Doping Graphene Transistors Using Vertical Stacked Monolayer WS <sub>2</sub> Heterostructures Grown by Chemical Vapor Deposition. ACS Applied Materials & Interfaces, 2016, 8, 1644-1652.	8.0	61
161	Biexciton Formation in Bilayer Tungsten Disulfide. ACS Nano, 2016, 10, 2176-2183.	14.6	57
162	Mixed multilayered vertical heterostructures utilizing strained monolayer WS <sub>2</sub> . Nanoscale, 2016, 8, 2639-2647.	5.6	27

#	Article	IF	CITATIONS
163	Torsional Deformations in Subnanometer MoS Interconnecting Wires. Nano Letters, 2016, 16, 1210-1217.	9.1	30
164	Electroluminescence Dynamics across Grain Boundary Regions of Monolayer Tungsten Disulfide. ACS Nano, 2016, 10, 1093-1100.	14.6	31
165	Elongated Silicon–Carbon Bonds at Graphene Edges. ACS Nano, 2016, 10, 142-149.	14.6	20
166	Mechanisms of monovacancy diffusion in graphene. Chemical Physics Letters, 2016, 648, 161-165.	2.6	24
167	Redox-Dependent Franck–Condon Blockade and Avalanche Transport in a Graphene–Fullerene Single-Molecule Transistor. Nano Letters, 2016, 16, 170-176.	9.1	93
168	Electron Exit Wave Reconstruction From a Single Defocused Image Using a Gaussian Basis. Microscopy and Microanalysis, 2015, 21, 745-746.	0.4	1
169	Detailed Atomic Structure of Defects in 2D Materials: From Graphene to Transition Metal Dichalcogenides. Microscopy and Microanalysis, 2015, 21, 573-574.	0.4	Ο
170	Three-terminal graphene single-electron transistor fabricated using feedback-controlled electroburning. Applied Physics Letters, 2015, 107, .	3.3	22
171	Uniformity of large-area bilayer graphene grown by chemical vapor deposition. Nanotechnology, 2015, 26, 395601.	2.6	21
172	High-quality functionalized few-layer graphene: facile fabrication and doping with nitrogen as a metal-free catalyst for the oxygen reduction reaction. Journal of Materials Chemistry A, 2015, 3, 15444-15450.	10.3	53
173	Resilient High Catalytic Performance of Platinum Nanocatalysts with Porous Graphene Envelope. ACS Nano, 2015, 9, 5947-5957.	14.6	55
174	Temperature dependence of atomic vibrations in mono-layer graphene. Journal of Applied Physics, 2015, 118, .	2.5	18
175	Conductance enlargement in picoscale electroburnt graphene nanojunctions. Proceedings of the National Academy of Sciences of the United States of America, 2015, 112, 2658-2663.	7.1	98
176	Layer-Dependent Modulation of Tungsten Disulfide Photoluminescence by Lateral Electric Fields. ACS Nano, 2015, 9, 2740-2748.	14.6	50
177	Controlled formation of closed-edge nanopores in graphene. Nanoscale, 2015, 7, 11602-11610.	5.6	38
178	Rotating Anisotropic Crystalline Silicon Nanoclusters in Graphene. ACS Nano, 2015, 9, 9497-9506.	14.6	15
179	Graphene-porphyrin single-molecule transistors. Nanoscale, 2015, 7, 13181-13185.	5.6	97
180	Atomic Level Distributed Strain within Graphene Divacancies from Bond Rotations. ACS Nano, 2015, 9, 8599-8608.	14.6	21

#	Article	IF	CITATIONS
181	Controlled Preferential Oxidation of Grain Boundaries in Monolayer Tungsten Disulfide for Direct Optical Imaging. ACS Nano, 2015, 9, 3695-3703.	14.6	119
182	All Chemical Vapor Deposition Growth of MoS <sub>2</sub> :h-BN Vertical van der Waals Heterostructures. ACS Nano, 2015, 9, 5246-5254.	14.6	326
183	Temperature Dependence of the Reconstruction of Zigzag Edges in Graphene. ACS Nano, 2015, 9, 4786-4795.	14.6	68
184	Enhanced spectroscopic gas sensors using <i>in-situ</i> grown carbon nanotubes. Applied Physics Letters, 2015, 106, .	3.3	26
185	Two-dimensional materials under electron irradiation. MRS Bulletin, 2015, 40, 29-37.	3.5	54
186	Transfer Printed Silver Nanowire Transparent Conductors for PbS–ZnO Heterojunction Quantum Dot Solar Cells. ACS Applied Materials & Interfaces, 2015, 7, 6417-6421.	8.0	21
187	Atomic Structure of Graphene Subnanometer Pores. ACS Nano, 2015, 9, 11599-11607.	14.6	75
188	Characterization of Graphene and Transition Metal Dichalcogenide at the Atomic Scale. Journal of the Physical Society of Japan, 2015, 84, 121005.	1.6	6
189	<i>In Situ</i> Observations of Free-Standing Graphene-like Mono- and Bilayer ZnO Membranes. ACS Nano, 2015, 9, 11408-11413.	14.6	118
190	Thermally Induced Dynamics of Dislocations in Graphene at Atomic Resolution. ACS Nano, 2015, 9, 10066-10075.	14.6	36
191	Formation of Klein Edge Doublets from Graphene Monolayers. ACS Nano, 2015, 9, 8916-8922.	14.6	9
192	Partial Dislocations in Graphene and Their Atomic Level Migration Dynamics. Nano Letters, 2015, 15, 5950-5955.	9.1	37
193	Spatially Dependent Lattice Deformations for Dislocations at the Edges of Graphene. ACS Nano, 2015, 9, 656-662.	14.6	12
194	Detailed formation processes of stable dislocations in graphene. Nanoscale, 2014, 6, 14836-14844.	5.6	29
195	Wired Up: Interconnecting Two-Dimensional Materials with One-Dimensional Atomic Chains. ACS Nano, 2014, 8, 11907-11912.	14.6	27
196	Extended Klein Edges in Graphene. ACS Nano, 2014, 8, 12272-12279.	14.6	41
197	Graphene for improved femtosecond laser based pluripotent stem cell transfection. Journal of Biophotonics, 2014, 7, 351-362.	2.3	2
198	Highly Electron Transparent Graphene for Field Emission Triode Gates. Advanced Functional Materials, 2014, 24, 1218-1227.	14.9	49

#	Article	IF	CITATIONS
199	Optically enhanced charge transfer between C <sub>60</sub> and single-wall carbon nanotubes in hybrid electronic devices. Nanoscale, 2014, 6, 572-580.	5.6	9
200	PbTe Nanocrystal Arrays on Graphene and the Structural Influence of Capping Ligands. Chemistry of Materials, 2014, 26, 1567-1575.	6.7	11
201	Hydrogen-free graphene edges. Nature Communications, 2014, 5, 3040.	12.8	74
202	Inflating Graphene with Atomic Scale Blisters. Nano Letters, 2014, 14, 908-914.	9.1	37
203	Shape Evolution of Monolayer MoS <sub>2</sub> Crystals Grown by Chemical Vapor Deposition. Chemistry of Materials, 2014, 26, 6371-6379.	6.7	698
204	Stability and Spectroscopy of Single Nitrogen Dopants in Graphene at Elevated Temperatures. ACS Nano, 2014, 8, 11806-11815.	14.6	45
205	Controlling sulphur precursor addition for large single crystal domains of WS <sub>2</sub> . Nanoscale, 2014, 6, 12096-12103.	5.6	149
206	Atomic Level Spatial Variations of Energy States along Graphene Edges. Nano Letters, 2014, 14, 6155-6159.	9.1	33
207	Nanoscale control of graphene electrodes. Physical Chemistry Chemical Physics, 2014, 16, 20398-20401.	2.8	67
208	Interactions of Pb and Te atoms with graphene. Dalton Transactions, 2014, 43, 7442-7448.	3.3	11
209	The Role of the Bridging Atom in Stabilizing Odd Numbered Graphene Vacancies. Nano Letters, 2014, 14, 3972-3980.	9.1	44
210	Crack-Free Growth and Transfer of Continuous Monolayer Graphene Grown on Melted Copper. Chemistry of Materials, 2014, 26, 4984-4991.	6.7	54
211	Stability and Dynamics of the Tetravacancy in Graphene. Nano Letters, 2014, 14, 1634-1642.	9.1	68
212	In situ observations of Pt nanoparticles coalescing inside carbon nanotubes. RSC Advances, 2014, 4, 49442-49445.	3.6	6
213	The development of a 200kV monochromated field emission electron source. Ultramicroscopy, 2014, 140, 37-43.	1.9	46
214	Atomic Structure and Dynamics of Metal Dopant Pairs in Graphene. Nano Letters, 2014, 14, 3766-3772.	9.1	219
215	Applications of Aberration Corrected TEM and Exit Wavefunction Reconstruction to Materials Science. Microscopy and Microanalysis, 2014, 20, 930-931.	0.4	0
216	Atomic Resolution Study of Defects in Graphene. Microscopy and Microanalysis, 2014, 20, 1766-1767.	0.4	0

#	Article	IF	CITATIONS
217	Surface energy-mediated construction of anisotropic semiconductor wires with selective crystallographic polarity. Scientific Reports, 2014, 4, 5680.	3.3	35
218	Reversible Loss of Bernal Stacking during the Deformation of Few-Layer Graphene in Nanocomposites. ACS Nano, 2013, 7, 7287-7294.	14.6	68
219	Sensitivity of Graphene Edge States to Surface Adatom Interactions. Nano Letters, 2013, 13, 4820-4826.	9.1	28
220	A graphene-based large area surface-conduction electron emission display. Carbon, 2013, 56, 255-263.	10.3	43
221	Bond Length and Charge Density Variations within Extended Arm Chair Defects in Graphene. ACS Nano, 2013, 7, 9860-9866.	14.6	38
222	Rippling Graphene at the Nanoscale through Dislocation Addition. Nano Letters, 2013, 13, 4937-4944.	9.1	59
223	Applications of Graphene. , 2013, , 333-437.		9
224	Properties of Graphene. , 2013, , 61-127.		9
225	Characterisation Techniques. , 2013, , 229-332.		8
226	Methods for Obtaining Graphene. , 2013, , 129-228.		13
227	Dynamics of Single Fe Atoms in Graphene Vacancies. Nano Letters, 2013, 13, 1468-1475.	9.1	228
228	Thin single-wall BN-nanotubes formed inside carbon nanotubes. Scientific Reports, 2013, 3, 1385.	3.3	58
229	Structural Reconstruction of the Graphene Monovacancy. ACS Nano, 2013, 7, 4495-4502.	14.6	131
230	Low temperature phase selective synthesis of Cu2ZnSnS4 quantum dots. Chemical Communications, 2013, 49, 3745.	4.1	52
231	Atomic resolution imaging of graphene by transmission electron microscopy. Nanoscale, 2013, 5, 4079.	5.6	125
232	Growth of carbon nanotubes via twisted graphene nanoribbons. Nature Communications, 2013, 4, 2548.	12.8	89
233	Carbon Nanomaterials: Synthesis, Properties and Applications. Nanoscience and Technology, 2012, , 23-46.	1.5	0
234	Synthesis of Adenine-Modified Reduced Graphene Oxide Nanosheets. Inorganic Chemistry, 2012, 51, 2954-2960.	4.0	60

#	Article	IF	CITATIONS
235	Synthesis of anisotropic PbS nanoparticles using heterocyclic dithiocarbamate complexes. Dalton Transactions, 2012, 41, 8297.	3.3	43
236	Visible light-driven CO <sub>2</sub> reduction by enzyme coupled CdS nanocrystals. Chemical Communications, 2012, 48, 58-60.	4.1	184
237	Pointwise Plucking of Suspended Carbon Nanotubes. Nano Letters, 2012, 12, 3663-3667.	9.1	5
238	Surfactant directed synthesis of calcium aluminum layered double hydroxides nanoplatelets. Journal of Materials Chemistry, 2012, 22, 7751.	6.7	33
239	Spatial control of defect creation in graphene at the nanoscale. Nature Communications, 2012, 3, 1144.	12.8	305
240	The Identification of Inner Tube Defects in Doubleâ€Wall Carbon Nanotubes. Small, 2012, 8, 3810-3815.	10.0	5
241	Shape and property control of Mn doped ZnSe quantum dots: from branched to spherical. Journal of Materials Chemistry, 2012, 22, 417-424.	6.7	24
242	Growth of Ultrahigh Density Single-Walled Carbon Nanotube Forests by Improved Catalyst Design. ACS Nano, 2012, 6, 2893-2903.	14.6	184
243	In-situ deposition of sparse vertically aligned carbon nanofibres on catalytically activated stainless steel mesh for field emission applications. Diamond and Related Materials, 2012, 23, 66-71.	3.9	14
244	Synthesis and separation of dyesvia Ni@reduced graphene oxide nanostructures. Journal of Materials Chemistry, 2012, 22, 1876-1883.	6.7	83
245	Atomic Structure of ABC Rhombohedral Stacked Trilayer Graphene. ACS Nano, 2012, 6, 5680-5686.	14.6	59
246	Optical studies of GaN nanocolumns containing InGaN quantum disks and the effect of strain relaxation on the carrier distribution. Physica Status Solidi C: Current Topics in Solid State Physics, 2012, 9, 712-714.	0.8	3
247	CVD rown Horizontally Aligned Singleâ€Walled Carbon Nanotubes: Synthesis Routes and Growth Mechanisms. Small, 2012, 8, 1973-1992.	10.0	49
248	Large Single Crystals of Graphene on Melted Copper Using Chemical Vapor Deposition. ACS Nano, 2012, 6, 5010-5017.	14.6	218
249	Dislocation-Driven Deformations in Graphene. Science, 2012, 337, 209-212.	12.6	332
250	Mechanical response of few-layer graphene films on copper foils. Scripta Materialia, 2012, 67, 273-276.	5.2	4
251	Aligned Rectangular Few-Layer Graphene Domains on Copper Surfaces. Chemistry of Materials, 2011, 23, 4543-4547.	6.7	51
252	Structural Distortions in Few-Layer Graphene Creases. ACS Nano, 2011, 5, 9984-9991.	14.6	29

#	Article	IF	CITATIONS
253	Motion of Light Adatoms and Molecules on the Surface of Few-Layer Graphene. ACS Nano, 2011, 5, 9428-9441.	14.6	26
254	Atomic Scale Growth Dynamics of Nanocrystals within Carbon Nanotubes. ACS Nano, 2011, 5, 1410-1417.	14.6	23
255	Ultralow Secondary Electron Emission of Graphene. ACS Nano, 2011, 5, 1047-1055.	14.6	72
256	Two-Dimensional Coalescence Dynamics of Encapsulated Metallofullerenes in Carbon Nanotubes. ACS Nano, 2011, 5, 10084-10089.	14.6	31
257	Atomic Structure of Interconnected Few-Layer Graphene Domains. ACS Nano, 2011, 5, 6610-6618.	14.6	77
258	Hexagonal Single Crystal Domains of Few-Layer Graphene on Copper Foils. Nano Letters, 2011, 11, 1182-1189.	9.1	289
259	Superparamagnetic Fe3O4 nanocrystals@graphene composites for energy storage devices. Journal of Materials Chemistry, 2011, 21, 5069.	6.7	336
260	3-Aryl-3-(trifluoromethyl)diazirines as Versatile Photoactivated "Linker―Molecules for the Improved Covalent Modification of Graphitic and Carbon Nanotube Surfaces. Chemistry of Materials, 2011, 23, 3740-3751.	6.7	32
261	Atomic Resolution Imaging of the Edges of Catalytically Etched Suspended Few-Layer Graphene. ACS Nano, 2011, 5, 1975-1983.	14.6	44
262	Internal Field Shielding and the Quantum Confined Stark Effect in a Single In[sub x]Ga[sub 1â^'x]N Quantum Disk. , 2011, , .		0
263	Optimizing substrate surface and catalyst conditions for high yield chemical vapor deposition grown epitaxially aligned single-walled carbon nanotubes. Carbon, 2011, 49, 5029-5037.	10.3	16
264	Reverse Micelle Synthesis of Coâ^'Al LDHs: Control of Particle Size and Magnetic Properties. Chemistry of Materials, 2011, 23, 171-180.	6.7	92
265	Noncovalent Binding of Carbon Nanotubes by Porphyrin Oligomers. Angewandte Chemie - International Edition, 2011, 50, 2313-2316.	13.8	90
266	Carbon nanotube nanoelectronic devices compatible with transmission electron microscopy. Nanotechnology, 2011, 22, 245305.	2.6	7
267	Utilizing boron nitride sheets as thin supports for high resolution imaging of nanocrystals. Nanotechnology, 2011, 22, 195603.	2.6	20
268	The catalytic potential of high-l $^{ m o}$ dielectrics for graphene formation. Applied Physics Letters, 2011, 98, .	3.3	63
269	Response to "Comment on â€~Ultrahigh secondary electron emission of carbon nanotubes' ―[Appl. Lett. 98, 066101 (2011)]. Applied Physics Letters, 2011, 98, .	Phys. 3.3	3
270	Optical studies on a single GaN nanocolumn containing a single InxGa1â^'xN quantum disk. Applied Physics Letters, 2011, 98, 251908.	3.3	6

#	Article	IF	CITATIONS
271	In-situ Observations of Restructuring Carbon Nanotubes via Low-voltage Aberration-corrected Transmission Electron Microscopy. Materials Research Society Symposia Proceedings, 2011, 1284, 101.	0.1	0
272	Carrier dynamics of InxGa1â^'xN quantum disks embedded in GaN nanocolumns. Journal of Applied Physics, 2011, 109, 063515.	2.5	9
273	Optical studies on In x Ga 1-x N quantum disks. Proceedings of SPIE, 2011, , .	0.8	0
274	Resolving strain in carbon nanotubes at the atomic level. Nature Materials, 2011, 10, 958-962.	27.5	61
275	Enhanced π-π interactions between a C60 fullerene and a buckle bend on a double-walled carbon nanotube. Nano Research, 2010, 3, 92-97.	10.4	16
276	Bioinspired Peonyâ€Like βâ€Ni(OH) <sub>2</sub> Nanostructures with Enhanced Electrochemical Activity and Superhydrophobicity. ChemPhysChem, 2010, 11, 489-494.	2.1	47
277	The formation of stacked-cup carbon nanotubes using chemical vapor deposition from ethanol over silica. Carbon, 2010, 48, 3175-3181.	10.3	29
278	Tracking down the catalytic hydrogenation of multilayer graphene. Physica Status Solidi C: Current Topics in Solid State Physics, 2010, 7, 2731-2734.	0.8	3
279	Exchange interactions of spin-active metallofullerenes in solid-state carbon networks. Physical Review B, 2010, 81, .	3.2	8
280	Single-wall-carbon-nanotube/single-carbon-chain molecular junctions. Physical Review B, 2010, 81, .	3.2	49
281	Publisher's Note: Single-wall-carbon-nanotube/single-carbon-chain molecular junctions [Phys. Rev. B <b>81</b> , 085439 (2010)]. Physical Review B, 2010, 81, .	3.2	0
282	Structural transformations of carbon chains inside nanotubes. Physical Review B, 2010, 81, .	3.2	15
283	In situobservations of self-repairing single-walled carbon nanotubes. Physical Review B, 2010, 81, .	3.2	24
284	Electron spin coherence in metallofullerenes: Y, Sc, and <mml:math xmlns:mml="http://www.w3.org/1998/Math/MathML" display="inline"&gt;<mml:mrow><mml:msub><mml:mrow><mml:mtext>La@C</mml:mtext></mml:mrow><mml:m Physical Review B, 2010, 82, .</mml:m </mml:msub></mml:mrow></mml:math 	arow≻ <mn< td=""><td>າl:mໍ້ຄົ&gt;82</td></mn<>	າl:mໍ້ຄົ>82
285	Ultrahigh secondary electron emission of carbon nanotubes. Applied Physics Letters, 2010, 96, .	3.3	22
286	Examining the stability of folded graphene edges against electron beam induced sputtering with atomic resolution. Nanotechnology, 2010, 21, 325702.	2.6	26
287	Electron Paramagnetic Resonance Investigation of Purified Catalyst-free Single-Walled Carbon Nanotubes. ACS Nano, 2010, 4, 7708-7716.	14.6	29
288	Direct Imaging and Chemical Identification of the Encapsulated Metal Atoms in Bimetallic Endofullerene Peapods. ACS Nano, 2010, 4, 3943-3948.	14.6	17

#	Article	IF	CITATIONS
289	High-Performance Field Effect Transistors from Solution Processed Carbon Nanotubes. ACS Nano, 2010, 4, 6659-6664.	14.6	29
290	Controlling intermolecular spin interactions of La@C82 in empty fullerene matrices. Physical Chemistry Chemical Physics, 2010, 12, 1618.	2.8	17
291	Elastic Distortions of Carbon Nanotubes Induced by Chiral Fullerene Chains ACS Nano, 2010, 4, 4011-4016.	14.6	16
292	The Molecular Structure of Polymerâ´'Fullerene Composite Solar Cells and Its Influence on Device Performance. Macromolecules, 2010, 43, 2343-2348.	4.8	65
293	Direct Low-Temperature Nanographene CVD Synthesis over a Dielectric Insulator. ACS Nano, 2010, 4, 4206-4210.	14.6	311
294	In situ observations of fullerene fusion and ejection in carbon nanotubes. Nanoscale, 2010, 2, 2077.	5.6	17
295	The influence of the number of graphene layers on the atomic resolution images obtained from aberration-corrected high resolution transmission electron microscopy. Nanotechnology, 2010, 21, 255707.	2.6	19
296	Atomic Resolution Imaging and Topography of Boron Nitride Sheets Produced by Chemical Exfoliation. ACS Nano, 2010, 4, 1299-1304.	14.6	337
297	Examining Co-Based Nanocrystals on Graphene Using Low-Voltage Aberration-Corrected Transmission Electron Microscopy. ACS Nano, 2010, 4, 470-476.	14.6	48
298	One-Dimensional Confined Motion of Single Metal Atoms inside Double-Walled Carbon Nanotubes. Physical Review Letters, 2009, 102, 195504.	7.8	38
299	Quantum confined Stark effect and corresponding lifetime reduction in a single InxGa1â^'xN quantum disk. Applied Physics Letters, 2009, 95, .	3.3	11
300	Capturing the Motion of Molecular Nanomaterials Encapsulated within Carbon Nanotubes with Ultrahigh Temporal Resolution. ACS Nano, 2009, 3, 3037-3044.	14.6	25
301	Superstructures of PbS nanocrystals in a conjugated polymer and the aligning role of oxidation. Nanotechnology, 2009, 20, 445608.	2.6	12
302	Shedding light on the crystallographic etching of multi-layer graphene at the atomic scale. Nano Research, 2009, 2, 695-705.	10.4	72
303	On the catalytic hydrogenation of graphite for graphene nanoribbon fabrication. Physica Status Solidi (B): Basic Research, 2009, 246, 2540-2544.	1.5	25
304	Structural transformations in graphene studied with high spatial and temporal resolution. Nature Nanotechnology, 2009, 4, 500-504.	31.5	203
305	Examining the Edges of Multi-Layer Graphene Sheets. Chemistry of Materials, 2009, 21, 2418-2421.	6.7	36
306	Acetylene: A Key Growth Precursor for Single-Walled Carbon Nanotube Forests. Journal of Physical Chemistry C, 2009, 113, 17321-17325.	3.1	120

#	Article	IF	CITATIONS
307	A bimetallic endohedral fullerene: PrSc@C80. Chemical Communications, 2009, , 4082.	4.1	15
308	Investigating the Diameter-Dependent Stability of Single-Walled Carbon Nanotubes. ACS Nano, 2009, 3, 1557-1563.	14.6	82
309	Investigating the Graphitization Mechanism of SiO <sub>2</sub> Nanoparticles in Chemical Vapor Deposition. ACS Nano, 2009, 3, 4098-4104.	14.6	89
310	Unravelling the Mechanisms Behind Mixed Catalysts for the High Yield Production of Single-Walled Carbon Nanotubes. ACS Nano, 2009, 3, 3839-3844.	14.6	3
311	Direct Imaging of Rotational Stacking Faults in Few Layer Graphene. Nano Letters, 2009, 9, 102-106.	9.1	225
312	Carbon nanotubes for interconnects in VLSI integrated circuits. Physica Status Solidi (B): Basic Research, 2008, 245, 2303-2307.	1.5	11
313	La@C <sub>82</sub> as a spinâ€active filling of SWCNTs: ESR study of magnetic and photophysical properties. Physica Status Solidi (B): Basic Research, 2008, 245, 2042-2046.	1.5	8
314	Selfâ€Assembly of Ligandâ€Free PbS Nanocrystals into Nanorods and Their Nanosculpturing by Electronâ€Beam Irradiation. Advanced Materials, 2008, 20, 784-787.	21.0	40
315	Biomolecule-Assisted Synthesis of Water-Soluble Silver Nanoparticles and Their Biomedical Applications. Inorganic Chemistry, 2008, 47, 5882-5888.	4.0	116
316	Rotating Fullerene Chains in Carbon Nanopeapods. Nano Letters, 2008, 8, 2328-2335.	9.1	57
317	Amino-acid-assisted synthesis and size-dependent magnetic behaviors of hematite nanocubes. Applied Physics Letters, 2008, 92, .	3.3	40
318	Crystallization and Self-Assembly of Calcium Carbonate Architectures. Crystal Growth and Design, 2008, 8, 4583-4588.	3.0	42
319	Dynamics of Paramagnetic Metallofullerenes in Carbon Nanotube Peapods. Nano Letters, 2008, 8, 1005-1010.	9.1	48
320	Grating of single Lu@C82 molecules using supramolecular network. Chemical Communications, 2008, , 4616.	4.1	19
321	Shape control of PbS nanocrystals using multiple surfactants. Nanotechnology, 2008, 19, 305605.	2.6	36
322	Growth and characterization of high-density mats of single-walled carbon nanotubes for interconnects. Applied Physics Letters, 2008, 93, 163111.	3.3	55
323	The synthesis of silicon and germanium quantum dots for biomedical applications. , 2006, , .		3
324	Synthesis of water-soluble photoluminescent germanium nanocrystals. Nanotechnology, 2006, 17, 3745-3749.	2.6	51

#	Article	IF	CITATIONS
325	Monodisperse PbS nanocrystals synthesized in a conducting polymer. Materials Letters, 2006, 60, 2375-2378.	2.6	19
326	Non-linear photoluminescence from purified aqueous PbS nanocrystals. Materials Letters, 2006, 60, 3332-3334.	2.6	16
327	Controlled formation of 3D CdS nanocrystal superlattices in solution. Nanotechnology, 2006, 17, 3035-3038.	2.6	15
328	Solution-phase synthesis of germanium nanoclusters using sulfur. Nanotechnology, 2006, 17, 5613-5619.	2.6	12
329	Photonics of silicon nanocrystals. , 2005, 6038, 254.		1
330	The synthesis of silicon nanoparticles for biomedical applications (Invited Paper). , 2005, , .		4
331	Water-Soluble Photoluminescent Silicon Quantum Dots. Angewandte Chemie - International Edition, 2005, 44, 4550-4554.	13.8	483
332	Synthesis and Self-Assembly of Triangular and Hexagonal CdS Nanocrystals. Advanced Materials, 2005, 17, 2997-3001.	21.0	91
333	Controlling PbS nanocrystal aggregation in conducting polymers. Nanotechnology, 2005, 16, 2381-2384.	2.6	28
334	Lead sulfide nanocrystal: conducting polymer solar cells. Journal Physics D: Applied Physics, 2005, 38, 2006-2012.	2.8	147
335	Surface Morphology Dependent Photoluminescence from Colloidal Silicon Nanocrystals. Journal of Physical Chemistry B, 2005, 109, 19064-19067.	2.6	101
336	Micro-emulsion synthesis of monodisperse surface stabilized silicon nanocrystals. Chemical Communications, 2005, , 1833.	4.1	191
337	Separating fluorescent species of aqueous PbS semiconductor nanocrystals using micro-emulsions. Nanotechnology, 2005, 16, 479-483.	2.6	10
338	Energy Transfer Dynamics of Nanocrystalâ^'Polymer Composites. Journal of Physical Chemistry B, 2005, 109, 9001-9005.	2.6	58
339	Time-resolved photoluminescence spectroscopy of ligand-capped PbS nanocrystals. Nanotechnology, 2005, 16, 175-179.	2.6	142
340	Direct observation of mixed-parity excited states in surface-passivated PbS nanocrystals. Nanotechnology, 2004, 15, 1351-1355.	2.6	5
341	Evidence for energy relaxation via a radiative cascade in surface-passivated PbS quantum dots. Nanotechnology, 2004, 15, 1328-1337.	2.6	16
342	Investigation of the role of cadmium sulfide in the surface passivation of lead sulfide quantum dots. Journal of Crystal Growth, 2004, 270, 380-383.	1.5	11

#	Article	IF	CITATIONS
343	Inorganic surface passivation of PbS nanocrystals resulting in strong photoluminescent emission. Nanotechnology, 2003, 14, 991-997.	2.6	54